

RAT LIVER NUCLEAR SKELETON AND RIBONUCLEOPROTEIN COMPLEXES CONTAINING HNRNA

THOMAS E. MILLER, CHEN-YA HUANG, and A. OSCAR POGO

From the Laboratory of Cell Biology, The Lindsley F. Kimball Research Institute of The New York Blood Center, New York, New York 10021. Dr. Miller's present address is the Department of Pathology and Laboratory Medicine, The Hahnemann Medical College and Hospital of Philadelphia, Philadelphia, Pennsylvania 19102.

ABSTRACT

Rat liver nuclei deprived of chromatin and nucleoplasm show a spongelike network which preserves its connection with nucleoli, the inner membrane of the nuclear envelope, and nuclear pore complexes. It contains all of the HnRNA, provided the endogenous proteolytic activity is inhibited by a proteolytic inhibitor such as phenylmethyl sulfonyl chloride (PMSC) or the fluoride form (PMSF). In the absence of these proteolytic inhibitors, HnRNA is dissociated from the spongelike network and sediments in a sucrose gradient as polydispersed ribonucleoprotein complexes. Furthermore, purified HnRNA as well as rRNA do not bind to the spongelike network when added to these nuclei. These observations demonstrate that the association of HnRNA to the nuclear skeleton is not an artifact. RNase treatment of the spongelike network digests the majority of the rapidly labeled RNA but does not alter the morphological aspect nor the architecture of this network. EDTA and heparin treatments affect neither the attachment of HnRNA nor the structural organization of this network. Electron microscope studies of the network reveal a characteristic flexuous configuration. Its relationship with diffused and condensed chromatin is discussed.

KEY WORDS nuclear skeleton · nuclear proteases · ribonucleoprotein complexes · heterogeneous RNA

From our studies on rat liver and ascites tumor nuclei, evidence has been obtained that ribonucleoprotein (RNP) complexes containing rapidly labeled RNA (HnRNA and presumably mRNA) are part of an RNP-network which in turn appears to be tightly bound to the nuclear envelope (11). Dissolution of this envelope by nonionic detergent does not release labeled RNA (11). Aaronson and Blobel (1) and Scheer and co-workers (32)

have found that similar treatment removes lipids from the nuclear envelope and that such membrane-denuded nuclei retain both their shape and pore complexes. They reported that these nuclear pore complexes are attached to intranuclear structures, particularly to a distinct peripheral layer of ill-defined nuclear material which they have interpreted as equivalent to the fibrous lamina described in a variety of cell types (14, 30, 33, 35). Berezney and Coffey have shown that a residual nuclear structure which preserves the nuclear shape remains after rat liver nuclei are treated with high salt and digested with ribonucle-

ase and deoxyribonuclease (3). A similar nuclear skeleton or matrix has been obtained from HeLa cells (21, 31), Chinese hamster cells (22), chicken erythrocytes (24), and *Tetrahymena* (37).

Nuclear disruption by a drastic mechanical procedure, such as sonication (34) or high pressure in a French pressure cell (11, 12), causes fragmentation of the RNP-network into a series of poly-dispersed RNP complexes of different size. It then became obvious that RNP complexes containing rapidly labeled RNA, nuclear skeleton, and the fibrous lamina with the pore complexes must be components of a unique nuclear structure.

In this report we wish to present biochemical and ultrastructural studies of a rat liver nuclear structure which is devoid of chromatin but is interconnected with nucleoli, nuclear pore complexes, and the inner membrane of the nuclear envelope, and contains all the rapidly labeled RNA. These studies strongly suggest that protein-protein and RNA-protein interactions are responsible for maintaining the RNP complexes that contain rapidly labeled RNA associated with the nuclear skeleton. This structure, located in the interchromatinic spaces, has a characteristic flexuous configuration.

MATERIALS AND METHODS

Isolation of Labeled Rat Liver Nuclei

Female rats (175–200 g) were labeled by intraperitoneal injection of 250 μ Ci of [3 H] orotic acid (sp act, 15–30 Ci/mmol; Amersham/Searle Corp., Arlington Heights, Ill.). After a period of 30 min, or in some experiments 5 min, the animals were sacrificed and the rat liver nuclei were isolated as reported earlier (11).

Isolation of a Nuclear Structure Containing Rapidly Labeled RNA

The extraction of chromatin with high salt buffer and DNase was a modification of the method of Faiferman and Pogo (11). Isolated nuclei were washed three times in 40 vol of a buffer solution containing 25 mM Tris-HCl, pH 7.5 (23°C), 2.5 mM MgCl₂, 0.25 M sucrose (TMS) with phenylmethyl sulfonyl chloride (PMSC), or the fluoride form, at a concentration of 0.5 mM. The PMSC was stored at –20°C in EtOH at a concentration of 0.1 M and dissolved in the buffer just before use. The final nuclear pellet was resuspended in 10 or 2.5 vol of a low salt buffer solution, which contained 0.1 M NaCl, 5 mM MgCl₂, 25 mM Tris-HCl, pH 7.6 (23°C), and 0.5 mM PMSC. To aliquots of 1 ml, 1 ml of a buffer containing 0.9 M NaCl, 5 mM MgCl₂, 25 mM

Tris-HCl, pH 7.6 (23°C), and 0.5 mM PMSC was added, giving a final ratio of packed nuclei to extraction buffer of either 1:20 or 1:5; the final concentration of this high salt buffer (HSB) was 0.5 N NaCl. This was gently stirred with a glass rod to homogenize the viscous nuclear suspension. The suspension was incubated with 300 μ g of DNase at 37°C and mixed with a Pasteur pipette until the suspension was no longer viscous. For the suspension at 1:20 it took about 30 s of incubation time, and for the suspension at 1:5 it took almost 2 min. The nuclei were counted in a hemacytometer before addition of HSB and after incubation to quantitate the number of nuclei which survived this treatment. A brief centrifugation (7 min at 1,000 g) of the digest resulted in a small, compact pellet at the bottom and a very loose, fluffy layer on top. The latter was gently resuspended with the supernate and centrifuged to equilibrium in a 30–68% sucrose gradient, which had a 72.5% sucrose to serve as a cushion (1 ml for 14-ml gradients, SW40-41 rotor, or 5 ml for 38-ml gradients, SW27 rotor). The gradients contained HSB buffer solution (0.5 M NaCl, 5 mM MgCl₂, and 25 mM Tris-HCl, pH 7.6, 23°C). The gradients were fractionated in an ISCO gradient fractionator (ISCO (Instrumentation Specialties Co.), Lincoln, Nebr.) with a UV absorption recorder, 254 μ m, 1-cm path length. To each fraction, 5 ml of 10% cold trichloroacetic acid was added and the acid-insoluble material was collected on a glass fiber filter (Whatman GF/B, Whatman, Inc., Clifton, N. J.), washed several times with 10% cold trichloroacetic acid, and radioactivities were determined by counting in Triton X-100-toluene solution (1:2, vol/vol) in a scintillation counter.

Ribonuclease Treatment of the Nuclear Structure Containing Rapidly Labeled RNA

The fraction of the sucrose gradient containing rapidly labeled RNA was collected. To 1.5 ml of this fraction, 3.5 ml of a buffer solution containing 25 mM Tris-HCl, pH 7.6, 23°C, 5 mM MgCl₂, and 0.5 mM PMSC was added and mixed. To this suspension, RNase was added as explained in the respective figures. This was incubated at 37°C for 5 min. Controls were incubated without RNase. The suspension was made 0.5 M NaCl and centrifuged in a 30–68% sucrose gradient as explained in the respective figures. The gradients were fractionated as previously explained.

Sodium Deoxycholate, EDTA, and Heparin Treatment

These treatments were similar to the RNase treatment, except that HSB buffer solution was used for dilution. (For EDTA treatment, HSB buffer solution contained no MgCl₂.) The samples were incubated at

0°C for at least 20 min before centrifugation in the 30–68% sucrose gradient.

Chemical Analysis

DNA was estimated by the diphenylamine reaction (6). RNA was determined by the method of Fleck and Munro (16), and protein was determined by the Lowry et al. procedure (26). Phospholipid phosphorus was estimated after extraction of the phospholipid according to Folch (17), and phosphate was determined by the method of Bartlett (2).

Determination of the Amount of UV

Absorption Material after Sucrose

Gradient Fractionation

A paper tracing procedure was used to measure the amount of UV absorption material sedimenting in different fractions of the sucrose gradient. Absorbance profiles were drawn on crystalline II guideline paper (Keuffel & Esser Co., Morristown, N. J.), cut as indicated in the respective figures, and weighed on a Mettler balance (Mettler Instrument Corp., Princeton, N. J.).

Extraction of Rapidly Labeled RNA

Species from Ascites Tumor Cells

Ascites tumor cells adapted to grow in vitro were maintained at a density of $5-8 \times 10^5$ cells/ml in Joklik medium (Spinner). For labeling, the cells were concentrated at a density of 2.0×10^6 /ml in Eagle's minimum essential medium supplemented with 10% dialyzed fetal calf serum and maintained in this medium for 1 h. Then 50 μ Ci of [5,6-³H]uridine (sp act, 46 Ci/mmol) was added to 20 ml of the cell suspension, and 7 min later the suspension was rapidly poured into 6 vol of semi-frozen, crushed 0.9% NaCl solution and was collected by centrifugation at 800 g for 7 min, washed once with the same solution, and then resuspended in 1 ml of a buffer containing 10 mM Tris-HCl, pH 7.9 (23°C), 1.5 mM MgCl₂, and 0.3 M sucrose. The cell suspension was frozen at -20°C and thawed before phenol extraction. To the thawed cell suspension, 0.1 vol of $\times 10$ NET buffer (1.0 M NaCl, 0.1 M EDTA, and 0.1 M Tris-HCl, pH 7.4, 23°C) was added. Three times the volume of $\times 1$ NET buffer was added, and the final suspension was made 0.2% with sodium dodecyl sulfate. An equal volume of freshly distilled phenol-cresol, containing 0.08% hydroxyquinoline, was added and vigorously stirred at 23°C for 20 min. The aqueous and phenol phases were separated by centrifugation; the aqueous phase was made 0.5 M with LiCl and reextracted with the phenol-cresol-hydroxyquinoline mixture. The aqueous phase was separated by centrifugation and the extracted RNA was precipitated with 2.5 vol of alcohol. After two washings with ethanol, the precipitated RNA was dissolved in double-distilled water. No DNA is extracted under these conditions.

Electron Microscopy

Suspensions of HSB-DNase-PMSC-treated nuclei, before centrifugation in the sucrose gradient, and nuclei sedimenting in the sucrose gradient were fixed with 4 vol of a fixative solution containing 4% glutaraldehyde, 2.5% formaldehyde, and 0.1 M Na cacodylate buffer, pH 7.2, at 4°C for 20 min. They were then centrifuged at 2,000 g for 30 min and the pellet was postfixed with 1% osmium tetroxide buffered with 0.1 M Na cacodylate, pH 7.2 at 4°C for 1 h. The specimens were dehydrated with acetone and embedded in Epon 812 mixture. Thin sections were double-stained with uranyl acetate and lead citrate solutions. Electron micrographs were made with a Philips 201 electron microscope at an original magnification ranging from $\times 3,000$ to $\times 70,000$.

RESULTS

Isolation of a Nuclear Structure

Containing Rapidly Labeled RNA

The method of isolating the nuclear structure that contains HnRNA and presumably mRNA species is based on three observations: (a) that rat liver chromatin can be unfolded and extracted at 0.5 M NaCl in the presence of 5 mM MgCl₂ and at pH 8.1,¹ a condition less likely to extract those elements of the nuclei associated with rapidly labeled RNA; (b) that this HSB-DNase treatment, although it digests the unfolded DNA and disintegrates the nucleosome (11), neither fragments the nuclei nor extracts all internal structures from the nuclei in the presence of a proteolytic inhibitor such as PMSC or PMSF; and (c) that equilibrium centrifugation in a 30–68% sucrose gradient separates the nuclear elements containing rapidly labeled RNA from the majority (mainly chromatin) of the UV-absorbing material of the nuclei.

The experiments shown in Fig. 1 demonstrated that when the treated nuclei are fractionated by this sucrose gradient the rapidly labeled RNA is located in three main fractions: one sedimenting on top of the gradient with the major UV-absorbing material, a second, which is polydisperse, sedimenting in the middle with two minor UV-absorbing materials (peaks I and II), and the third sedimenting near the bottom at a density of 1.25 g/ml which coincides with a prominent and well-defined UV-absorbing material (peak III). The nuclear material sedimenting in peak III can be seen as a turbid, well-defined layer, sometimes a

¹ The pH of 25 mM Tris-HCl at 4°C.

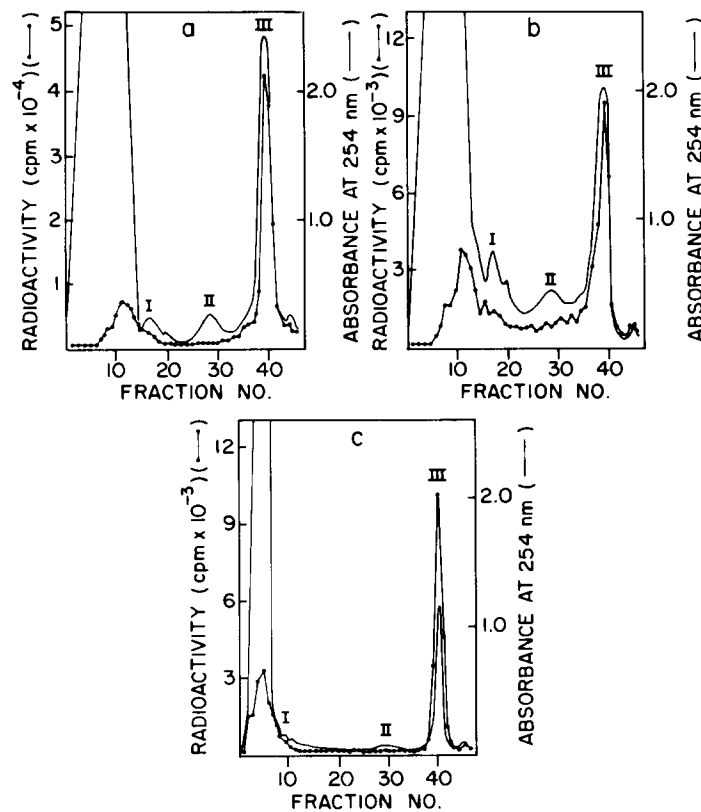


FIGURE 1 Sucrose gradient centrifugation of nuclei treated by the HSB-DNase method in the presence of the proteolytic inhibitor PMSC. Rats were injected with [³H]orotic acid, and nuclei were isolated and treated as explained in Materials and Methods. Chromatin extraction was performed in the presence of 0.5 mM PMSC at a ratio of 20 vol of buffer to 1 vol of packed nuclei. The 1,000 g supernate was layered on a 30–68% sucrose gradient containing 1 ml of 72.5% sucrose as a cushion. In (a) labeling was carried out for 30 min and in (b) for 5 min. 0.8 ml of each supernate was layered and centrifuged in the Spinco SW 41 rotor at 36,000 rpm for 18 h. In (c) the labeling was carried out for 30 min, and 0.2 ml of the supernate was layered and centrifuged in the Spinco SW41 rotor at 18,000 rpm for 18 h. The gradients were fractionated and radioactivities determined as explained in Materials and Methods. The direction of sedimentation is from left to right.

bilayer. This pattern of UV and radioactive profiles does not change when the time of labeling is decreased to 5 min or when the centrifugal force is reduced to one-fourth (Fig. 1b and c). The perfect coincidence between UV-absorbing material and rapidly labeled RNA when conditions of centrifugation and labeling are changed indicates that (a) the rapidly labeled RNA is attached to structures of different sedimentation rates, the one which is in peak III being the most rapidly sedimenting material, and that (b) the fractionation does not differentiate between structures containing nascent RNA and rapidly labeled RNA.

The most interesting feature of this fractionation is the labeling of the prominent peak III

which does not change its position when it sediments at high or low centrifugal force. It is concluded that both labeled RNA and the UV-absorbing material are in the same nuclear structure. The experiments described in Fig. 1 rule out the possibility that the radioactive profile could be caused by very dense structures sedimenting at this position, whereas the UV profile is caused by structures that have reached equilibrium at this position. In general, the amount of radioactive RNA and UV-absorbing material recovered in peak III correlates with nuclear survival. Hemacytometer counting before and after treatment indicates that 50–80% of the nuclei survive the chromatin extraction, a fractional value which is

similar to the amount of radioactivity recovered in peak III. Nuclear survival is probably a function of the condition of the isolated nuclei, the amount of mechanical injury they sustain during extraction and, most importantly, the efficiency of the proteolytic inhibitor. The latter is clearly demonstrated in the experiments described in Fig. 2.

In the absence of the inhibitor the radioactive profile is very heterodisperse. There is a dramatic reduction of the prominent peak III and a shift to the top of the gradient of the UV-absorbing material (Fig. 2). 0.1 mM PMSC gave a pattern similar to that without inhibitor, and 1.0 mM PMSC (data not shown) gave a pattern similar to that of 0.5 mM PMSC (Fig. 1a). The fluoride form of the inhibitor gave similar results, but the chloride form gave consistently higher yields. Experiments in which the proteolytic inhibitor benzamidine was used showed no improvement over experiments without any inhibitor, whereas in experiments in which the inhibitor *p*-toluene sulfonyl lysine chloromethyl ketone (TLCK) was used, the radioactive profiles resembled those

obtained with PMSC, but generally the profiles were more heterodisperse (data not shown).

The majority of DNA sediments on top of the sucrose gradient, hence the radioactive RNA found in this fraction would be nascent RNA still attached to the chromatin and different from the labeled RNA which sediments in the middle or at the bottom of the gradient (in peak III). One should then expect that, after a 5-min pulse of labeling, most of the radioactive RNA should sediment in the first 20 fractions. However, after a 5-min pulse, only 39% of the total radioactivity sediments in these first 20 fractions, and after a 30-min pulse, about 20–30% of the total radioactivity sediments in this region of the gradient (Fig. 1b, and c). The insignificant difference between 5- and 30-min pulses indicates that most of the radioactivity at the top of the gradient is derived from those nuclei that do not survive chromatin extraction. The increase in radioactivity in the first 20 fractions, the apparent shift to the top of the gradient of the UV-absorbing material from peak III, and the increase in polydisperse radioactive material when the chromatin is extracted in the absence of the proteolytic inhibitor strongly support this assumption (Fig. 2).

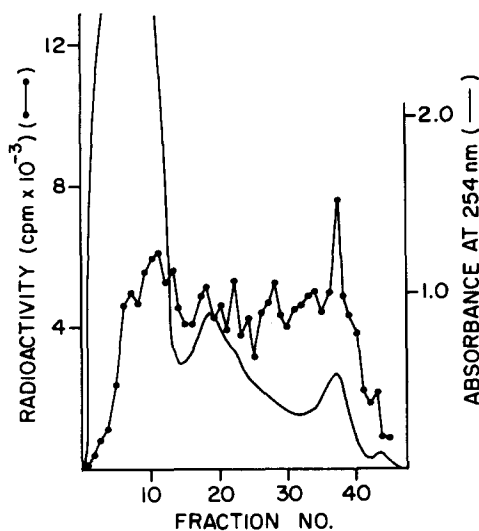


FIGURE 2 Sucrose gradient centrifugation of nuclei treated by the HSB-DNase method in the absence of the proteolytic inhibitor PMSC. Rats were injected with [^3H]orotic acid and nuclei were isolated and treated as explained in Materials and Methods but without PMSC. Chromatin extraction was performed without PMSC at a ratio of 5 vol of buffer to 1 vol of packed nuclei. 0.8 ml of the 1,000 g supernate was layered on a 30–68% sucrose gradient containing 1 ml of 72.5% sucrose as a cushion and centrifuged at 36,000 rpm for 18 h. The direction of sedimentation is from left to right.

Addition of Radioactive RNA to Treated Nuclei and to the Nuclear Structure that Sediments in Peak III

The possibility that rapidly labeled RNA *in vivo* is not bound to nuclear structures that sediment in peak III but becomes associated with them after the nuclei are treated with the high salt buffer and DNase is explored in the experiment shown in Fig. 3. As can be seen, low and high molecular weight RNAs² do not sediment in the same position as the nuclear structures, when added either to treated nuclei or to purified nuclear structures sedimenting in peak III. The sedimentation behavior of the labeled RNA did change, instead of sedimenting in a heterogeneous radioactive profile as in Fig. 3a (see inset), it sedimented to the bottom of the centrifuge tube when mixed with treated nuclei (Fig. 3b) or the nuclear structures sedimenting in peak III (Fig. 3c). This change is

² High molecular weight RNAs are HnRNA and 45S rRNA precursor. In the standard 15–30% sucrose gradient they sediment more rapidly than in the 30–68% sucrose gradient containing the high salt buffer (see Fig. 3a, insert).

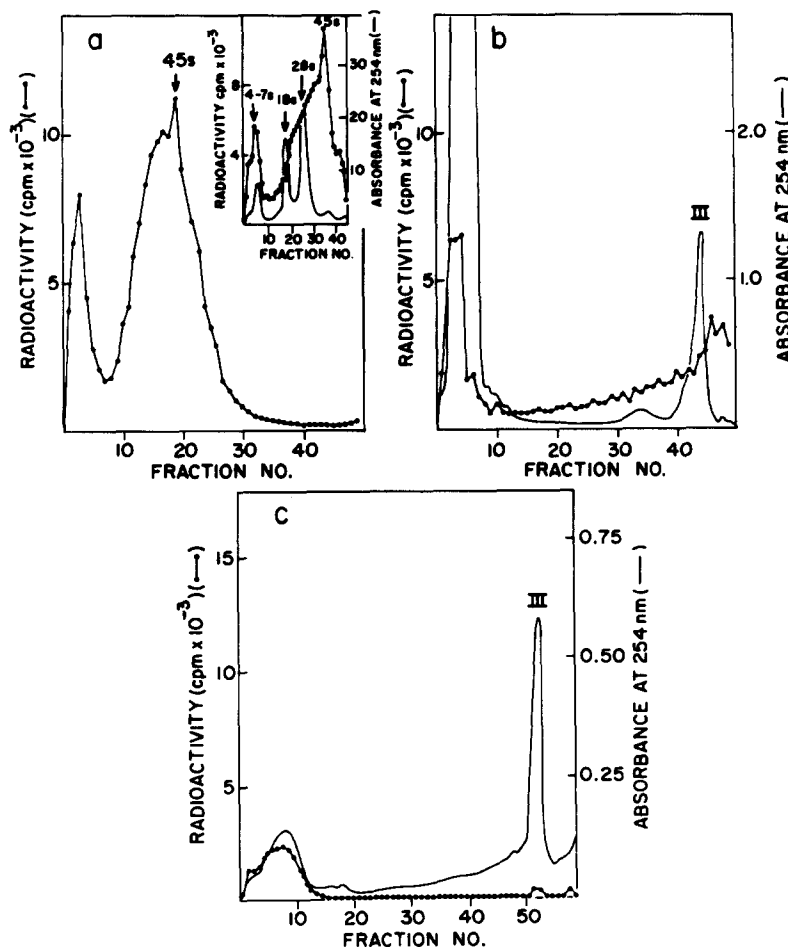


FIGURE 3 Sucrose gradient analysis of radioactive RNA added to the treated nuclei and to nuclei sedimented in peak III. (a) 200 μg of labeled RNA (2.1×10^5 cpm) was dissolved in HSB containing PMSC, layered onto the type of sucrose gradient described in Fig. 1, and centrifuged in the Spinco SW40 rotor at 18,000 rpm for 18 h. Inset is the same labeled RNA but layered on a 5–40% sucrose gradient containing 0.1 M NaCl, 0.05 M Na acetate, pH 5.1, and centrifuged at 26,000 rpm for 16 h. (b) 0.4 ml of nuclei, treated by the HSB-DNase-PMSC method as described in Fig. 1, was mixed with 0.1 ml of HSB containing PMSC, and 200 μg of labeled RNA (2.1×10^5 cpm). The mixture was layered onto a similar gradient and centrifuged as in (a). (c) The nuclear structure sedimenting in peak III (see Fig. 1) was isolated from the sucrose gradient, and 1.5 ml of this fraction was diluted with 3.5 ml of HSB containing PMSC, and to this 200 μg of labeled RNA (2.1×10^5 cpm) was added, and the mixture was layered on the type of sucrose gradient described in Fig. 1 and centrifuged in a Spinco SW27 rotor at 18,000 rpm for 18 h. The gradients were fractionated as explained in Materials and Methods, and radioactivity of each fraction was determined by counting directly in Scintisol (Isolab, Inc., Akron, Ohio). Radioactivities in pellets were: (a) 0.04×10^5 cpm; (b) 0.9×10^5 cpm; (c) 1.7×10^5 cpm. Recoveries of radioactivities from all gradients were $\sim 80\%$. The direction of sedimentation is from left to right.

probably due to the interaction of nuclear protein with the labeled RNA, causing either aggregation of this labeled RNA or producing a protein coat that increases its sedimentation rate. The experi-

ment explained in Fig. 3 demonstrates that the association between endogenous rapidly labeled RNA and the nuclear structure is not an artifact. It also proves that this RNA is not entrapped by

any nuclear structure which would cause it to be pushed along the gradient by the sedimenting structures.

Electron Microscope Studies of the Treated Nuclei

Electron microscope observations have revealed a characteristic spongelike skeletal network structure in all nuclei studied. Such a network was found throughout the whole nucleus and appears to have a close association with nucleoli, inner membrane of the nuclear envelope, and nuclear pore complexes (Figs. 4–6, and 8). However, some differences do exist in nuclei before and after sedimentation through the sucrose gradient. Thus, before this centrifugation some nuclei contain a diffuse material which we believe to be the unfolded and digested chromatin. There is a large variation in the amount of this chromatinic material, and there are nuclei which only contain large, empty spaces enclosed by the spongelike network (Fig. 4*a*).

It is suggested that a leaking out of chromatin has left these large spaces empty. Some nuclear ghosts or empty nuclear envelopes are also observed. Well-defined nucleoli and a largely well-preserved nuclear envelope with characteristic nuclear pore complexes are clearly seen in the majority of nuclei. The outer nuclear membrane seems to bleb, detach, and in some instances disappear.

After sucrose gradient centrifugation, the material which sediments in peak III is primarily composed of a nuclear structure devoid of diffuse chromatin (Fig. 4*b*). Nuclei with large empty spaces, a spongelike network, nucleoli, and nuclear envelope predominate in this fraction. The most distinguishing morphological feature of the nuclei sedimenting in this peak is the presence of a spongelike network and absence of the diffuse chromatinic material. We infer that they are "achromatinic nuclei." The small amount of material sedimenting in peaks I and II shows structures with similar morphology; although these nuclei contain less amounts of the network, many are without nucleoli and there are many empty nuclear envelopes or ghosts (not shown).

The detailed study of the spongelike network before and after centrifugation in the sucrose gradient (nuclei sedimenting in peak III) reveals components of different electron densities (Fig.

5*a* and *b*). The less electron-dense structure is interspersed by clusters of heavier electron-dense structures. The less electron-dense structure is less visible after sedimentation throughout the sucrose gradient. Centrifugation most probably removes a large proportion of this structure (Fig. 5, compare *a* and *b*).

At high magnification, the more electron-dense material is a structure of flexuous or zigzag configuration. An interesting feature is the raggedness of its borderline. A similar rough borderline is also seen adjacent to the nucleolus and inner membrane of the nuclear envelope. Connections between the nuclear pore complexes and nucleolus are seen (Fig. 6*a* and *b*).

Chemical Composition

The distribution of phospholipids, proteins, RNA, and DNA in treated nuclei before and after purification (peak III) is shown in Table I. The achromatinic nuclei preparation (peak III) is rich in RNA and proteins (which probably accounts for its higher density) and is clearly different in chemical composition from the nuclear ghosts and/or nuclear membranes isolated by various laboratories (3, 24, 31, 38). In the same table, the recovery of all these components from the treated nuclei is shown. As monitored by chemical analysis, the nuclei deprived of chromatin retain 65% of the phospholipids, 31% RNA, 19% proteins, and 0.48% DNA. If one assumes that all the achromatinic nuclei contain membranes, then the percentage of total phospholipids found in peak III is a reflection of the percent of total nuclei which survive the treatment and purification throughout the sucrose gradient.³ One can then calculate the percentage of the components that are part of these achromatinic nuclei. From these calculations, about half of the nuclear RNA and about one-third of the total nuclear proteins are part of these nuclei. Furthermore, because in nuclei isolated by our method, half of the total proteins are histones, and because in the achromatinic nuclei all histones are released (11), one can assume that ~60% of the nonhistone proteins are recovered in these nuclei. The remainder of the nonhistone proteins of the nuclei may be either soluble proteins, some proteins released by the treatment, or both.

³ Recoveries monitored by counting, phospholipids, and radioactive RNA determination agree very well.

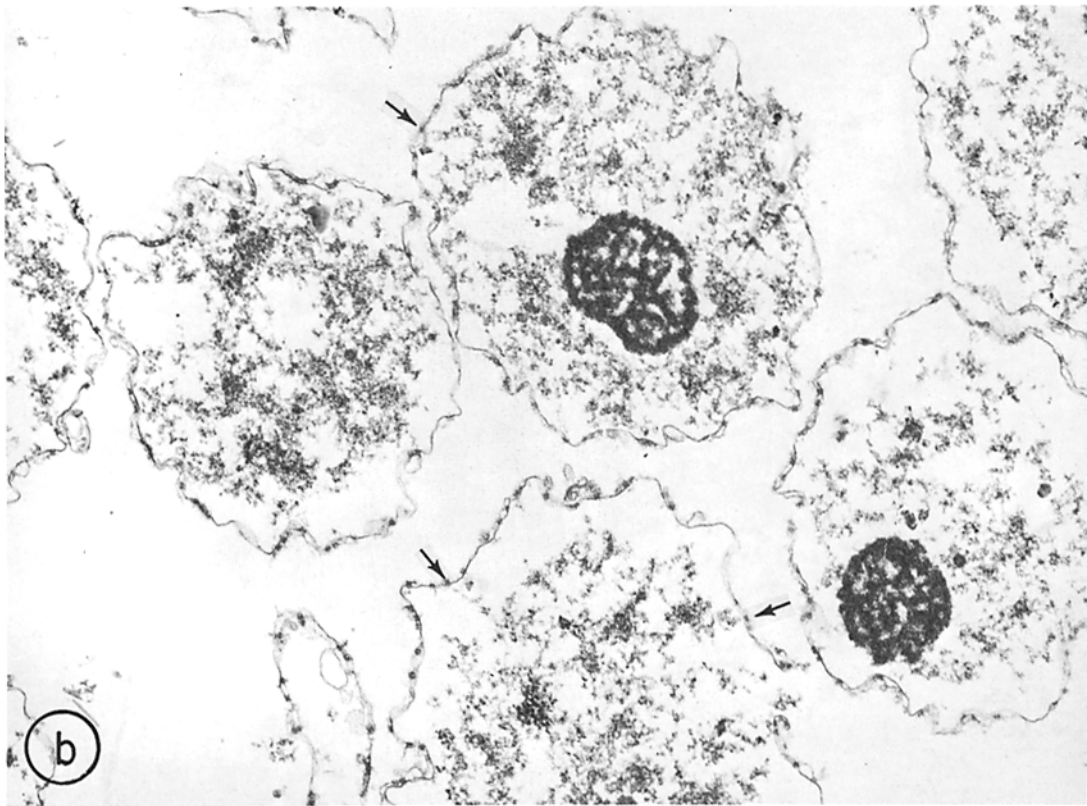
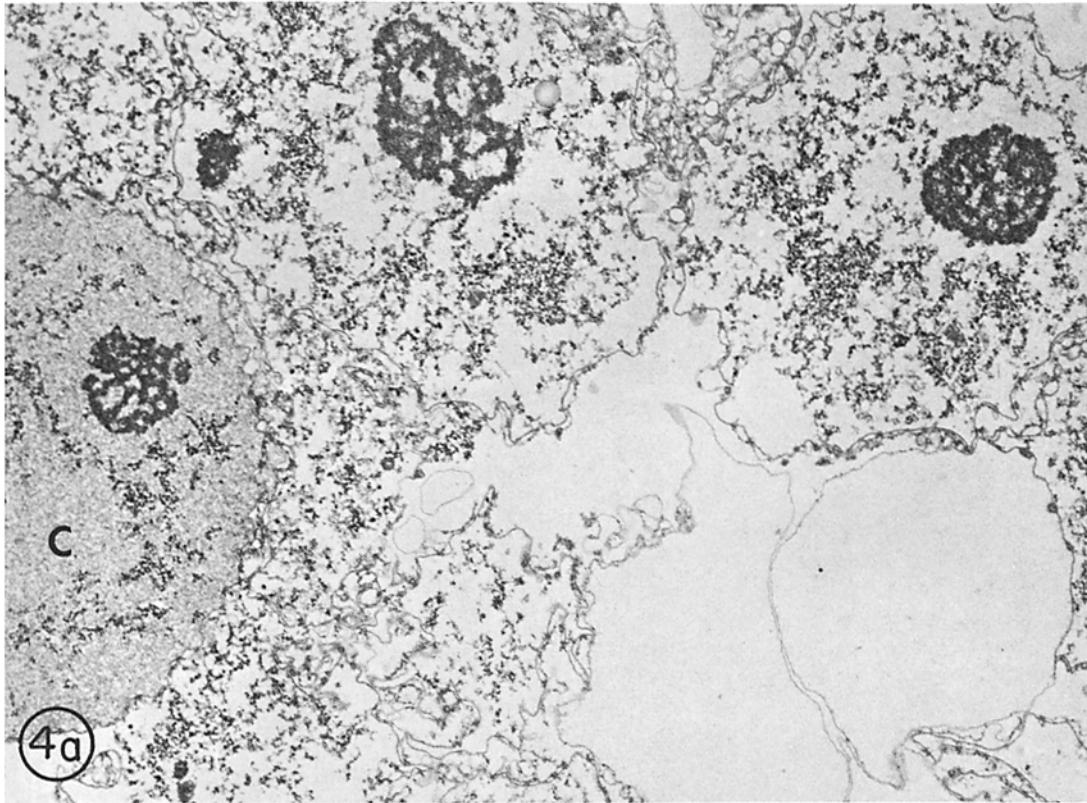


FIGURE 4 Rat liver nuclei treated by the HSB-DNase-PMSC method. (a) shows nuclei before sedimentation through the sucrose gradient. Unfolded chromatin and digested chromatin (C) are seen in a diffused form in a nucleus. (b) shows nuclei sedimenting in peak III of Fig. 1. A spongelike network and its connection with the nuclei, particularly with the nuclear pore complexes (arrows), are observed. $\times 9,000$.

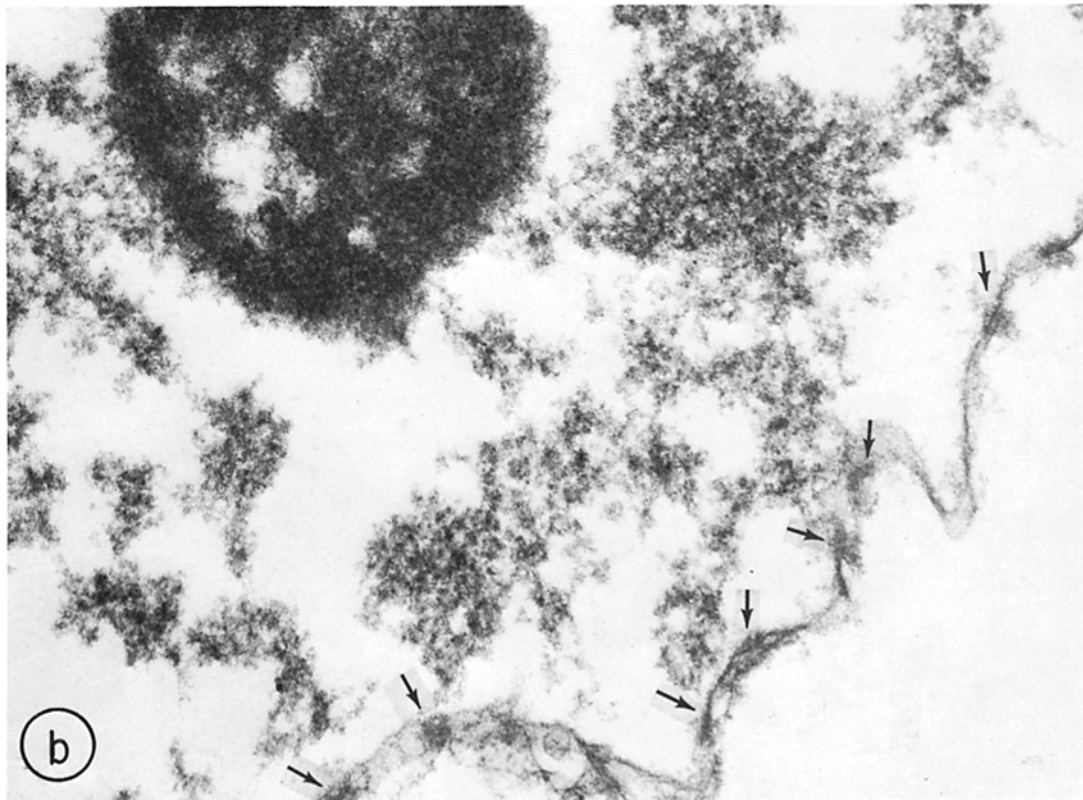
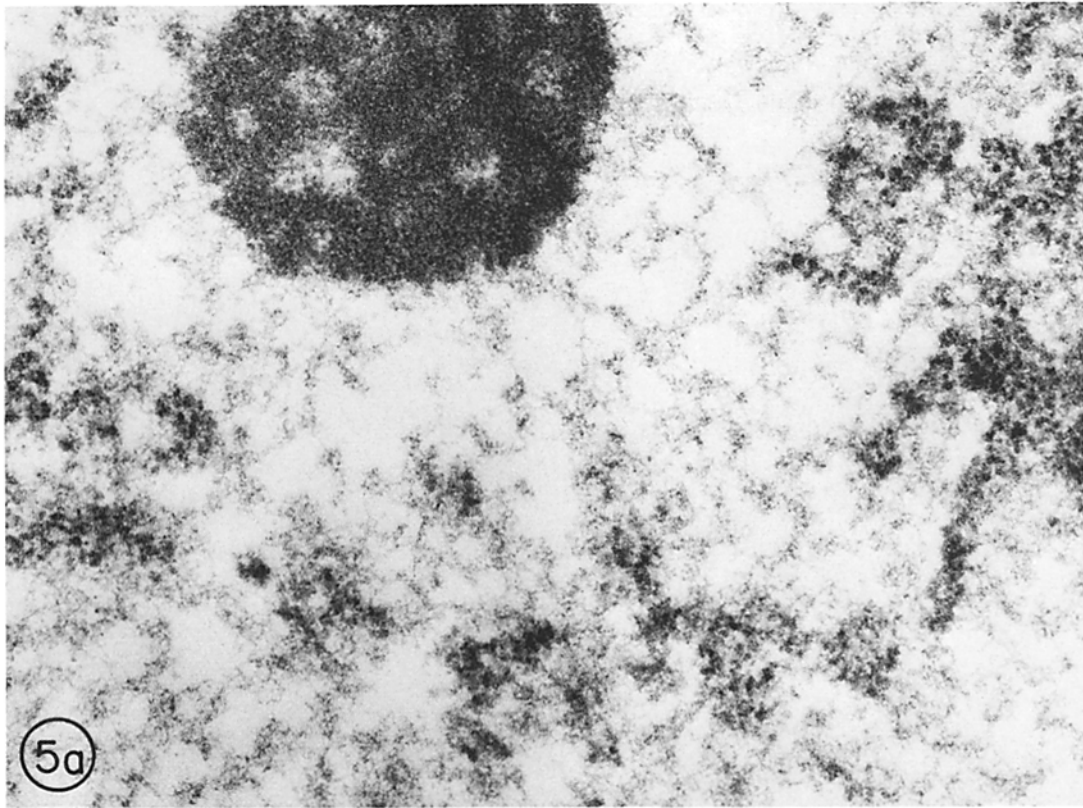


FIGURE 5 Higher magnification of a typical nucleus as seen in Fig. 4 *a* and *b*. (*a*) portion of a nucleus before sedimentation in the sucrose gradient. The spongelike network appears to consist of less electron-dense structures interspersed by clusters of heavier electron-dense structures. (*b*) portion of a typical nucleus sedimenting in peak III of Fig. 1. The heavier electron-dense structure is what primarily remains after sucrose gradient centrifugation. The general pattern of close association between the spongelike network and nuclear pore complexes (arrows) is indicated. $\times 45,000$.

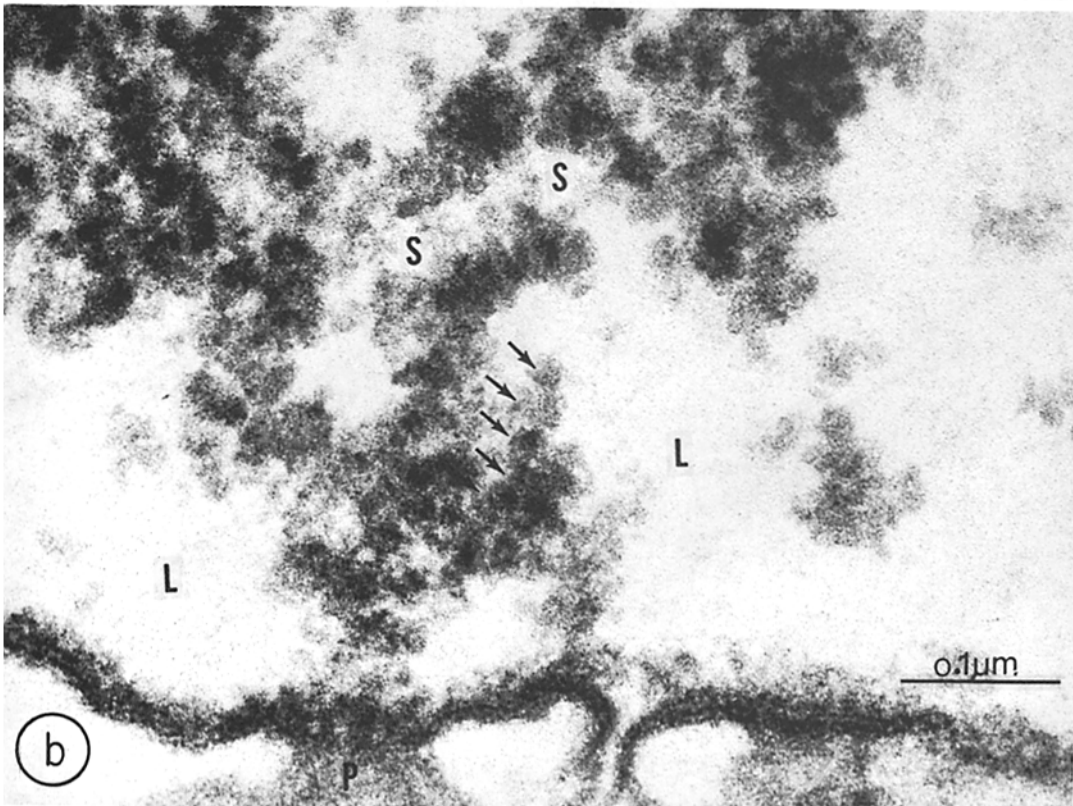
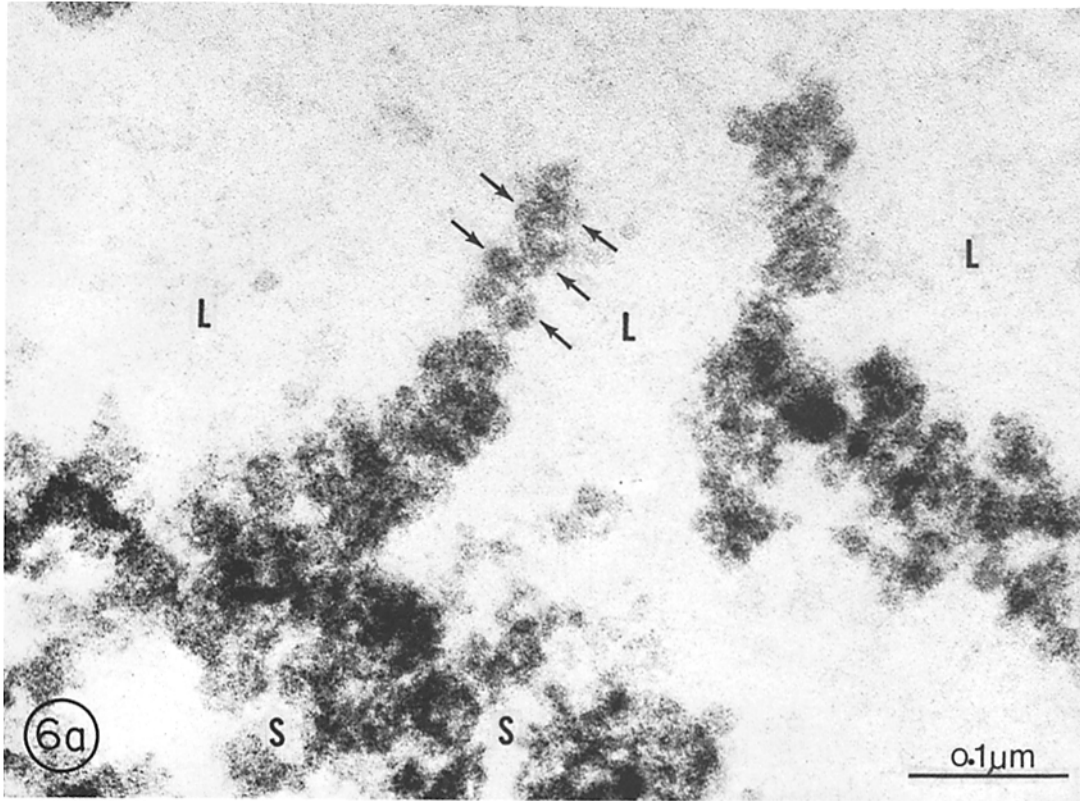


FIGURE 6 Fine structure of the spongelike network in nuclei sedimenting in peak III of Fig. 1. A flexuous or zigzag arrangement appears to be the general pattern of the heavier electron-dense structure. (a) a projection in a large empty space (*L*) is shown. This zigzag configuration is also seen in small empty spaces (*S*). These spaces, within and around the electron-dense network frames, could be the spaces left over by chromatin or some other nuclear components. (b) a direct connection with nuclear pore complexes (*P*) is often seen. $\times 210,000$.

TABLE I
DNA, RNA, Proteins and Phospholipids in Nuclei, Treated Nuclei, and Achromatic Nuclei

	DNA		RNA		Protein		Phospholipids	
	pg*	Recovery from nuclei§ %	pg	%	pg	%	pg	%
Nuclei	11.75 (11.7-11.8)	—	1.93 (1.76-2.10)	5.2	23.0 (22.9-23.2)	61.5	0.71 (0.56-0.87)	1.9
Treated nuclei	4.7 (4.5-4.9)	39	1.92 (1.75-2.10)	6.3	23.0 (22.9-23.1)	75.8	0.70 (0.56-0.85)	2.3
Achromatic nuclei (peak III)	0.057 (0.059-0.055)	0.48	0.59 (0.61-0.58)	11.0	4.3 (4.5-4.1)	79.5	0.46 (0.41-0.52)	8.5
								65

Nuclei represent nuclei isolated from rat liver and washed with TMS as explained in Materials and Methods. Treated nuclei represent nuclei treated by the HSB-DNase-PMSC method. Achromatic nuclei represent nuclei sedimenting in peak III of Fig. 1.

* pg per each type of nuclei.

† DNA + RNA + proteins + phospholipids = 100%.

§ Amount recovered in treated nuclei and achromatic nuclei. The values are averages of two determinations.

Effect of Different Treatment on the Rapidly Labeled RNA Associated with Achromatinic Nuclei (Nuclei Sedimenting in Peak III)

Treatment of achromatinic nuclei with different concentrations of RNase removes the rapidly labeled RNA (Fig. 7). Only at high concentrations (5 $\mu\text{g}/\text{ml}$) does the density of these nuclei decrease (Fig. 7*d*). Because limiting RNase digestion produces neither a polydisperse radioactive profile

nor a shift of radioactivity to the top of the gradient, it is evident that the RNA has been digested *in situ* to very small molecules which become trichloroacetic soluble (see Fig. 7*c* and *d*). A decrease in UV absorbance in peak III, with an increase of this UV absorbance on top of the gradient when digestion has been carried out at high enzyme concentrations, indicates that components which are associated with RNA have been removed, and digestion also disintegrates some of the components of the achromatinic nuclei. Nevertheless, the radioactive RNA ap-

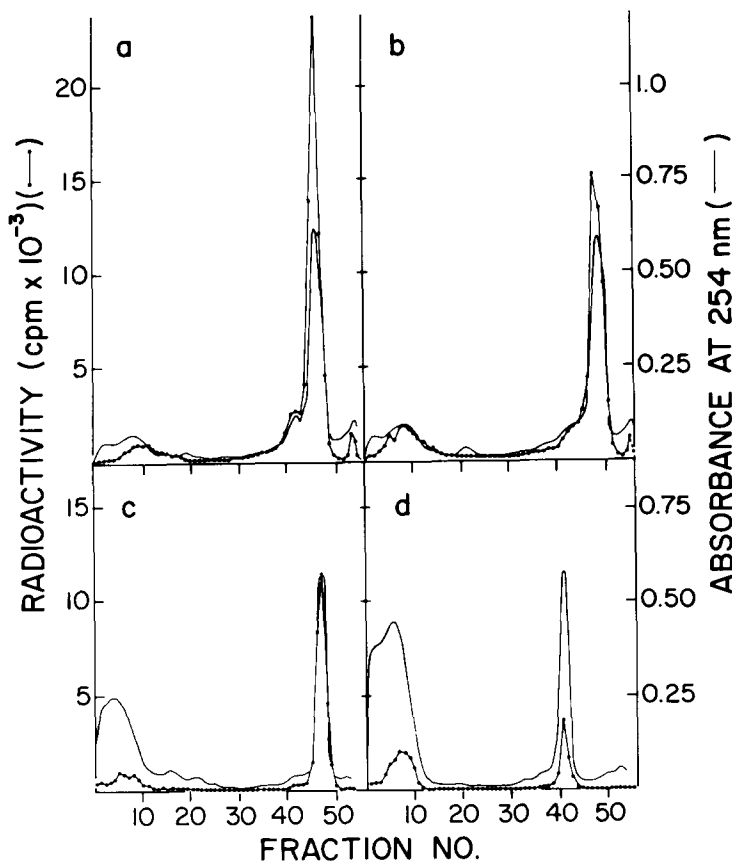


FIGURE 7 Effect of RNase treatment on the nuclear structure that sediments as peak III. The nuclear structure was isolated from sucrose gradients similar to the one explained in Fig. 1, except that the gradients were centrifuged in the Spinco SW27 rotor at 24,000 rpm for 18 h. Fractions of the gradient containing the nuclear structures were collected, pooled, and treated with different concentrations of pancreatic RNase as described in Material and Methods. (a) control rerun; (b) control incubation, the same as in (a) except that after dilution the isolated nuclear structures were incubated at 30°C for 5 min; (c) the same as (b) except that pancreatic RNase at a concentration of 0.5 $\mu\text{g}/\text{ml}$ was added and the nuclear structures were incubated as before; (d) same as (c) except that RNase was at a concentration of 5.0 $\mu\text{g}/\text{ml}$. The sucrose gradients were centrifuged in the Spinco SW27 rotor at 24,000 rpm for 19 h, and radioactivity was determined as explained in Materials and Methods. The direction of sedimentation is from left to right.

pears to be the component most sensitive to enzyme digestion. This can be seen in Fig. 7*d* where a prominent UV-absorbing peak coincides with very little labeled RNA. The recovery of radioactivity in the digested achromatinic nuclei decreases as follows: 75% for those nondigested and incubated, 34% for those digested with 0.5 $\mu\text{g/ml}$ of RNase, and 12% for those digested with 5.0 $\mu\text{g/ml}$ of RNase. However, the amount of UV-absorbing material recovered in peak III is 75% in nuclei nondigested but incubated, 67% in those digested with 0.5 $\mu\text{g/ml}$ of RNase, and 41% in those digested with 5.0 $\mu\text{g/ml}$ of RNase. This experiment indicates (*a*) that there is some digestion of rapidly labeled RNA by endogenous ribonucleases, and (*b*) that the radioactive RNA is highly sensitive to either endogenous or exogenous RNase digestion.

Heparin treatment at a concentration of 0.4 $\mu\text{g/ml}$, which has been claimed to remove nuclear RNA (4), has little, if any, effect on both UV absorbance and radioactive patterns (not shown). However, sodium deoxycholate at very low concentrations (0.05%) removes radioactive RNA (trichloroacetic-soluble) from the achromatinic nuclei which, devoid of the nuclear envelope, sediment to the bottom of the tube (not shown). In the pellet, the amount of radioactive RNA rendered trichloroacetic insoluble decreases with increasing concentration of sodium deoxycholate. Thus, 37, 17, and 9% of the radioactivity are recovered in this pellet when achromatinic nuclei are treated with 0.05, 0.2, and 0.5% sodium deoxycholate, respectively (not shown). This effect is similar to that observed in RNP complexes isolated by compression and decompression in a French pressure cell (12).

Treatment of achromatinic nuclei with 5 mM and 10 mM EDTA gave UV absorbance and radioactive profiles identical with those of the control. It is obvious that divalent cations are not important for the interaction of rapidly labeled RNA nor for the assembly of the different components of these nuclei.

Finally, in Fig. 8*a* and *b* is shown the ultrastructure of those achromatinic nuclei which are devoid of rapidly labeled RNA and which sediment as a prominent UV absorption peak as shown in Fig. 7*d*. No morphologically identifiable gross difference between the treated and untreated achromatinic nuclei can be seen, nor do the nucleoli show any sign of disintegration after this RNase digestion.

DISCUSSION

The study reported in this paper demonstrates that RNP complexes which contain rapidly labeled RNA are naturally attached to the nuclear skeleton. It also shows that this association cannot be generated as a result of adventitious RNA-protein interactions. This possibility is very unlikely, for radioactive RNA added before or after purification does not bind to achromatinic nuclei (Fig. 3).

The fact that inhibition of proteases is essential to prevent release of RNP complexes indicates that the so-called nuclear informosomes are produced to a large extent by proteolytic activity. A number of studies on chromatin-associated proteases capable of degrading histones have been reported (8, 10, 18). A general belief which has emerged from these studies is that the proteases found associated with chromatin are of nuclear origin. However, two recent studies have indicated that these nuclear proteases are of cytoplasmic origin, for rat liver chromatin can be isolated in the absence of the above proteolytic activity, provided the chromatin is isolated from purified nuclei rather than from tissue (9, 20). Because we extracted chromatin from nuclei purified through a high concentration of sucrose (a method which has been claimed to remove proteases of cytoplasmic origin [9, 20]), we believe that the proteolytic activities which remove the RNP complexes are of nuclear origin. The nature and specificity of these proteolytic activities remain to be established.

Nuclear proteolysis releases RNP complexes from the nuclear skeleton and converts achromatinic nucleic into nuclear ghosts or empty nuclear envelopes. Our interpretation of these phenomena is that protein-protein interactions are an important force which maintains the RNP complexes attached to the nuclear skeleton. Furthermore, digestion of certain proteins associated with the RNP complexes makes the RNA susceptible to nucleolytic attack, and hence RNA-protein interaction is the other force which maintains the RNP complexes bound to the nuclear skeleton. The experiments of limited RNase digestion support this assumption. This treatment not only solubilizes radioactive RNA, but reduces the density of achromatinic nuclei and converts many of them into nuclear skeletons. There is, however, a preferential solubilization of radioactive RNA over the conversion of achromatinic nuclei to nuclear ghosts. It follows that: (*a*) rapidly labeled RNA is readily susceptible to nucleolytic attack, and (*b*)

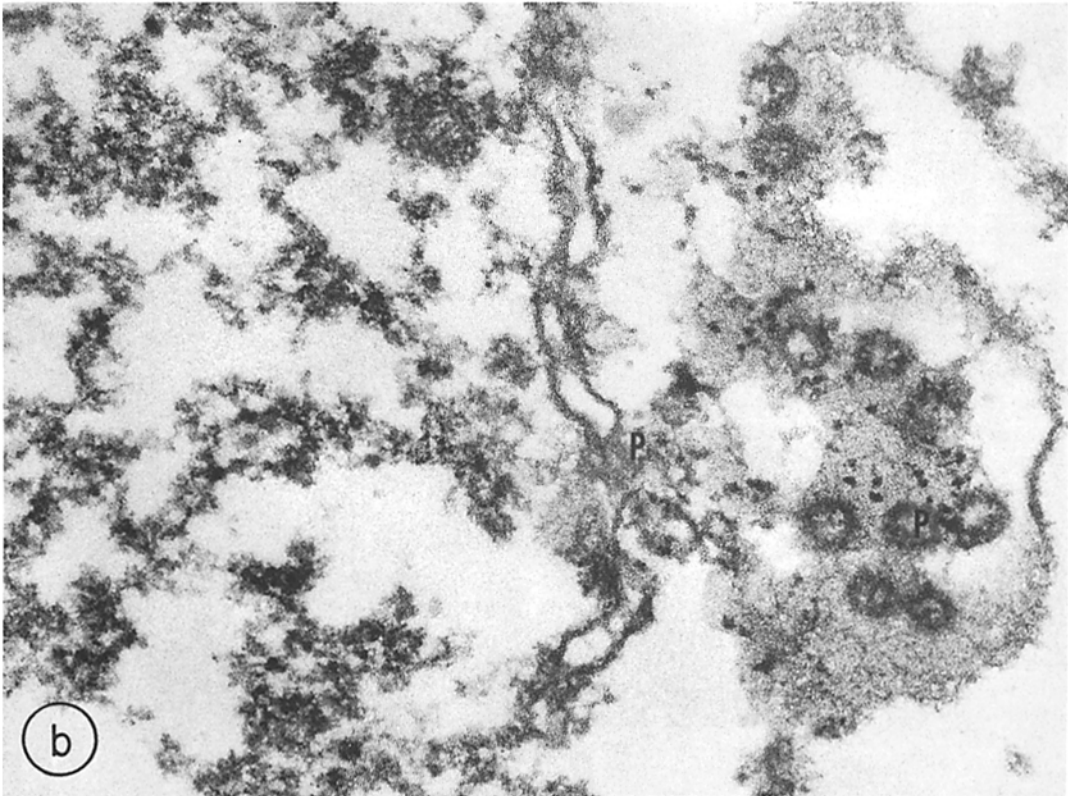
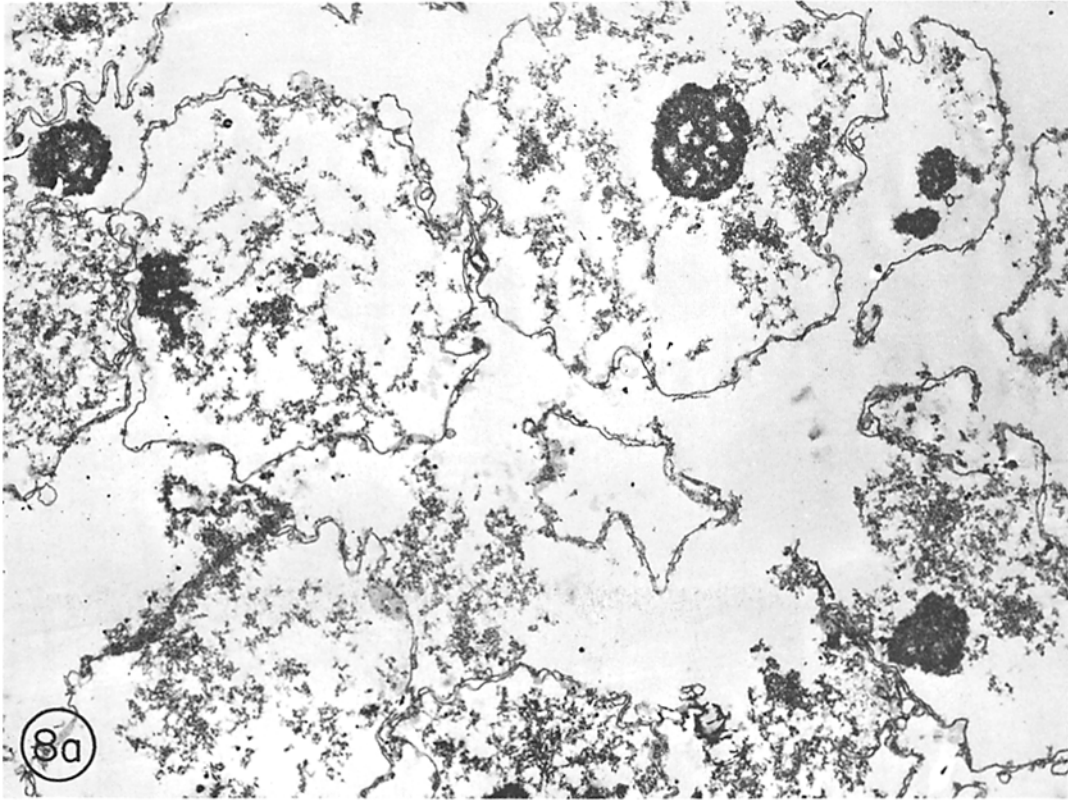


FIGURE 8 RNase-digested nuclei sedimenting in peak III of Fig. 7c. A similar spongelike network and its close association with nuclear pore complexes (*P*) are observed in spite of the removal of labeled RNA. (*a*), $\times 9,000$; (*b*), $\times 90,000$.

RNA species less accessible to nucleolysis are also components of the RNP complexes. In the following paper, we report on the presence of stable smwRNA species as components of the achromatic nuclei (28).

Because EDTA treatment neither affects the RNA complex nor converts achromatic nuclei into nuclear ghosts, the attachment of the RNP complexes to the nuclear skeleton is not mediated by divalent cations. The high susceptibility of achromatic nuclei and RNP complex to sodium deoxycholate may be due to detergent activation of endogenous proteolytic and nucleolytic activities, or the detergent may dissociate proteins from the RNP complexes. The latter suggests that proteins are bound to RNA by hydrophobic interaction (12).

No major alteration in the ultrastructure of RNase-treated achromatic nuclei is observed. However, a certain amount of RNase-digested achromatic nuclei sediments as lighter structures on top of the sucrose gradient. To obtain a nuclear skeleton or a nuclear envelope devoid of RNA, drastic RNase digestion and higher ionic strength are necessary (3, 21, 22, 31, 37, 38). In general, this structure also reveals a spongelike network, and its chemical analysis indicates a very low RNA content (3, 24, 31, 37, 38). As we have previously demonstrated, drastic RNase digestion is insufficient in eliminating all the elements of the network, whereas pronase digestion completely destroys the network (11). Although at the morphological level it is impossible to discern which elements of the RNP network are protein and which are RNP complexes, it is reasonable to assume that RNP complexes are associated with the nuclear skeleton of which protein may be its major component. This skeleton has connections with the nucleolus and the proteinaceous layer adjacent to the inner membrane of the nuclear envelope, i.e., the fibrous lamina (1, 14, 30, 32, 35). The ultrastructure of this network reveals a characteristic flexuous configuration, and at the present time, it is not clear whether this arrangement is due to a corrugated protein shell or to a helical protein fibril.

It is a well-known fact that DNA is not evenly distributed in rat liver nuclei nor in many other differentiated cells. There are regions of the nuclei around the nucleolus (perinucleolar chromatin) and adjacent to the nuclear envelope where DNA is highly concentrated, i.e., the compact chromatin (5). In other regions of the nuclei the chroma-

tin is diffuse; it is here where uptake of radioactive RNA precursor is much more pronounced (7, 13, 19, 23, 25). A remarkable feature of the achromatic nuclei is that the pattern distribution of the spongelike network is the reciprocal pattern of DNA distribution in intact nuclei. The concentration of the network diminished in those regions, around the nucleolus and adjacent to the inner membrane of the nuclear envelope, where condensed chromatin exist.

Is there any evidence that this structure actually exists in this configuration in the intact nuclei? The best evidence comes from the work of Bernhard and his colleagues (29) who have shown the presence of an interchromatin fibrogranular material when thin sections of tissue are treated with EDTA, a procedure which bleaches the chromatin. Furthermore, it has been recently reported that after a short labeling with radioactive RNA precursor, the radioactivity is predominantly associated with this fibrogranular material (13). It would seem reasonable to equate this fibrogranular material with the structure that we visualize in the achromatic nuclei. Allowing for the possibility of shrinkage and distortion in the specimens when prepared for the electron microscope, the structure in its native state should then follow the contours of the chromatin cables. However, to support this assumption, morphological evidence of this nature is not enough. Another important aspect of the structural organization of the nucleus has to be taken into consideration, the natural connection of RNP complexes with chromatin. When chromatin of *Drosophila melanogaster* embryos is spread, McKnight and Miller (27) observed that one end of nonnucleolar RNP fibrils is bound to chromatin. It then follows that attachment of RNP complexes to either chromatin or nuclear skeleton depends upon which of these two nuclear structures is preserved. Thus, when chromatin is digested, the RNP complexes remain bound to the nuclear skeleton. On the other hand, when the nuclear skeleton is dissolved by detergents, the RNP complexes remain attached to the chromatin cables (27). Because RNP complexes are not free in the nucleoplasm (11), it then follows that chromatin and the spongelike network of the nuclear skeleton must be close to one another. In other words, the structure that we observed in rat liver achromatic nuclei would follow the contours of the chromatin cables.

The new knowledge that emerges from recent studies of chromatin fibrils indicates a pattern of

DNA folding in a nucleohistone arrangement (nucleosomes) with two orders of coiling: the one around the nucleosome provides a coil of 100 Å diameter, a super-helix DNA-histone fibril, and the other a super-super helix or solenoid producing a 200–300 Å diameter chromatin cable (15). The super-super helix is stabilized by H1-H1 histone interactions (36). It is not fortuitous that spaces of 220 Å average (190–250 Å of 300 measured) are observed inside and along the heavier electron-dense structure. These spaces may correspond in intact nuclei to longitudinal or cross sections of a 200–300 Å diameter chromatin cable (Fig. 6a and b).

In any case, this material appears to be thin in condensed chromatin (high solenoid concentration) and very thick in diffused chromatin (low solenoid concentration). RNP complexes containing HnRNA are then attached to the spongelike network, and it is not clear, at this time, whether these complexes exist as folded or compact structures, or as fibrils stretched along the surface of the protein network. Whatever the configuration of the RNP complexes, it is evident that they do not contribute either to the morphological aspect or to the architecture of the nuclear skeleton. Moreover, rapidly labeled RNA, the majority of which is HnRNA, must be on the surface of a core structure formed by protein-protein interactions. We visualize two orders of structural organization. One is the nuclear skeleton or protein matrix, the other are RNP complexes containing rapidly labeled RNA.

We wish to thank Ms. Vivian Sarantis and Ms. Ruth Ann Gollobin for their skillful assistance.

This work was supported by grant HL-09011 from the National Heart and Lung Institute.

Reprint requests should be made to Dr. A. Oscar Pogo, The New York Blood Center, 310 East 67th St., New York, New York 10021.

Received for publication 13 July 1977, and in revised form 11 October 1977.

REFERENCES

1. AARONSON, R. P., and G. BLOBEL. 1975. Isolation of the nuclear pore complex in association with a lamina. *Proc. Natl. Acad. Sci. U. S. A.* **72**:1007–1011.
2. BARTLETT, C. R. 1959. Phosphorous assay in column chromatography. *J. Biol. Chem.* **234**:466–468.
3. BEREZNEY, R., and D. S. COFFEY. 1977. Nuclear matrix: isolation and characterization of a framework structure from rat liver nuclei. *J. Cell Biol.* **73**:616–637.
4. BORNENS, M. 1973. Action of heparin on nuclei: solubilization of chromatin enabling the isolation of nuclear membrane. *Nature (Lond.)*. **244**:28–30.
5. BOUTEILLE, M., M. LAVAL, and A. M. DUPUY-COIN. 1974. Localization of nuclear functions as revealed by ultrastructural autoradiography and cytochemistry. *In* The Cell Nucleus. H. Busch, editor. Academic Press, Inc., New York. **1**:3–71.
6. BURTON, K. 1956. A study of the conditions and mechanism of the diphenylamine reaction for the colorimetric estimation of deoxyribonucleic acid. *Biochem. J.* **62**:315–323.
7. CAMERON, I. L., and D. M. PRESCOTT. 1963. RNA and protein metabolism in the maturation of the nucleated chicken erythrocyte. *Exp. Cell Res.* **30**:609–612.
8. CHONG, M. T., W. T. GARRARD, and J. BONNER. 1974. Purification and properties of a neutral protease from rat liver chromatin. *Biochemistry*. **13**:5128–5134.
9. DESTREE, O. H. J., H. A. D'ADELHART-TOOROP, and R. CHARLES. 1975. Cytoplasmic origin of the so-called nuclear neutral histone protease. *Biochim. Biophys. Acta.* **378**:450–458.
10. EICKBUSCH, T., D. K. WATSON, and E. N. MOURDRIANAKIS. 1976. A chromatin-bound proteolytic activity with unique specificity for histone H2A. *Cell*. **9**:785–792.
11. FAIFERMAN, I., and A. O. POGO. 1975. Isolation of a nuclear ribonucleoprotein network that contains heterogeneous RNA and is bound to the nuclear envelope. *Biochemistry*. **14**:3808–3816.
12. FAIFERMAN, I., M. G. HAMILTON, and A. O. POGO. 1971. Nucleoplasmic ribonucleoprotein particles of rat liver II. Physical properties and action of dissociating agents. *Biochim. Biophys. Acta.* **232**:685–695.
13. FAKAN, S., E. PUVION, and G. SPOHR. 1976. Localization and characterization of newly synthesized nuclear RNA in isolated rat hepatocytes. *Exp. Cell Res.* **99**:155–164.
14. FAWCETT, D. W. 1966. On the occurrence of a fibrous lamina on the inner aspect of the nuclear envelope in certain cells of vertebrates. *Am. J. Anat.* **119**:129–146.
15. FINCH, J. T., and A. KLUG. 1976. Solenoidal model for superstructure in chromatin. *Proc. Natl. Acad. Sci. U. S. A.* **73**:1897–1901.
16. FLECK, A., and H. N. MUNRO. 1962. The precision of ultraviolet absorption measurements in the Schmidt-Thannhauser procedure for nucleic acid estimation. *Biochim. Biophys. Acta.* **55**:571–583.
17. FOLCH, J. 1952. The role of phosphorous in the metabolism of lipids. *In* Phosphorous Metabolism. W. D. McElroy and B. Glass, editors. The Johns

- Hopkins University Press, Baltimore, Md. 2:186-202.
18. FURLAN, M., and M. JERICIJO. 1967. Protein catabolism in thymus nuclei I. Hydrolysis of nucleoproteins by proteases present in calf-thymus nuclei. *Biochim. Biophys. Acta.* **147**:135-144.
 19. HARRIS, H. J. 1967. The reactivation of the red cell nucleus. *J. Cell Sci.* **2**:23-32.
 20. HEINRICH, P. C., G. RAYDT, B. PUSCHENDORF, and M. JUSIC. 1976. Subcellular distribution of histone-degrading enzyme activities from rat liver. *Eur. J. Biochem.* **62**:32-43.
 21. HERMAN, R., G. ZIEVE, J. WILLIAMS, R. LENK, and S. PENMAN. 1976. Cellular skeletons and RNA messages. In *Progress in Nucleic Acid Research and Molecular Biology*. W. E. Cohn and E. Volkin, editors. Academic Press, Inc., New York. **19**:379.
 22. HILDERRAND, C. E., R. T. OKINAKA, and L. R. C. GURLEY. 1975. Existence of a residual nuclear protein matrix in cultured chinese hamster cells. *J. Cell Biol.* **67**:169a (Abstr.).
 23. HSU, J. 1962. Differential rate in DNA synthesis between euchromatin and heterochromatin. *Exp. Cell Res.* **27**:332-334.
 24. JACKSON, B. 1976. Polypeptide of the nuclear envelope. *Biochemistry.* **15**:5641-5651.
 25. LITTAU, V. C., V. G. ALLFREY, J. H. FRENSTER, and A. E. MIRKSY. 1964. Active and inactive regions of nuclear chromatin as revealed by electron microscope autoradiography. *Proc. Natl. Acad. Sci. U. S. A.* **52**:93-100.
 26. LOWRY, O. H., N. J. ROSEBROUGH, A. L. FARR, and R. J. RANDALL. 1951. Protein measurement with the Folin phenol reagent. *J. Biol. Chem.* **193**:265-275.
 27. MCKNIGHT, S. L., and O. L. MILLER. 1976. Ultrastructural patterns of RNA synthesis during early embryogenesis of *Drosophila melanogaster*. *Cell.* **8**:305-319.
 28. MILLER, T. E., C.-Y. HUANG, and A. O. POGO. 1978. Rat liver nuclear skeleton and small molecular weight RNA species. *J. Cell Biol.* **76**:692-704.
 29. MONNERON, A., and W. BERNHARD. 1969. Fine structural organization of the interphase nucleus in mammalian cells. *J. Ultrastruct. Res.* **27**:266-288.
 30. PATRIZI, G., and M. POGER. 1967. The ultrastructure of the nuclear periphery. *J. Ultrastruct. Res.* **17**:127-136.
 31. RILEY, D. E., J. M. KELLER, and B. BYERS. 1975. The isolation and characterization of nuclear ghosts from cultured HeLa cells. *Biochemistry.* **14**:3005-3013.
 32. SCHEER, U., J. KARTENBECK, M. F. TRENDELENBURG, J. STADLER, and W. W. FRANKE. 1976. Experimental disintegration of the nuclear envelope. Evidence for pore-connecting fibrils. *J. Cell Biol.* **69**:1-18.
 33. STELLY, N. B., B. J. STEVENS, and J. ANDRÉ. 1970. Etude cytochimique de la lamelle dense de l'enveloppe nucleaire. *J. Microsc. (Paris).* **9**:1015-1028.
 34. STÉVENIN, J., H. GALLINARO-MATRINCE, R. GATTONI, and M. JACOB. 1977. Complexity of the structure of particles containing heterogeneous nuclear RNA as demonstrated by ribonuclease treatment. *Eur. J. Biochem.* **74**:589-602.
 35. STEVENS, B. J., and J. ANDRÉ. 1969. The Nuclear Envelope. In *Handbook of Molecular Cytology*. A. Lima-de-Faria, editor. North-Holland Publishing Co., Amsterdam. 837-871.
 36. WORCEL, A., and J. N. BENYAJATI. 1977. High order coiling of DNA in chromatin. *Cell.* **12**:83-100.
 37. WUNDERLICH, F., and A. HERLAN. 1977. A reversibly contractile nuclear matrix. Its isolation, structure and composition. *J. Cell Biol.* **73**:271-278.
 38. ZBARSKY, I. B., K. A. PEREVOSHCHIKOVA, L. N. DELEKTORSKAYA, and V. V. DELEKTORSKY. 1969. Isolation and biochemical characterization of the nuclear envelope. *Nature (Lond.).* **221**:257-259.